

<b>REPORT DOCUMENTATION PAGE</b>			Form Approved OMB No. 0704-0188	
Public reporting burden for this collection of information is estimated to average 1 hour per response, including the time for reviewing instructions, searching existing data sources, gathering and maintaining the data needed, and completing and reviewing the collection of information. Send comments regarding this burden estimate or any other aspect of this collection of information, including suggestions for reducing this burden, to Washington Headquarters Services, Directorate for Information Operations and Reports, 1215 Jefferson Davis Highway, Suite 1204, Arlington, VA 22202-4302, and to the Office of Management and Budget, Paperwork Reduction Project (0704-0188), Washington, D.C. 20503.				
<b>1. AGENCY USE ONLY (Leave blank)</b>		<b>2. REPORT DATE</b> July 1992	<b>3. REPORT TYPE AND DATES COVERED</b> Technical Memorandum	
<b>4. TITLE AND SUBTITLE</b> Effects of Fragmentation Parameter Variations on Estimates of Galactic Cosmic Ray Exposure <i>Dose Sensitivity Studies for Aluminum Shields</i>			<b>5. FUNDING NUMBERS</b>  WU 593-42-21-01	
<b>6. AUTHOR(S)</b> Lawrence W. Townsend, Francis A. Cucinotta, Judy L. Shinn, and John W. Wilson				
<b>7. PERFORMING ORGANIZATION NAME(S) AND ADDRESS(ES)</b> NASA Langley Research Center Hampton, VA 23665-5225			<b>8. PERFORMING ORGANIZATION REPORT NUMBER</b>  L-17082	
<b>9. SPONSORING/MONITORING AGENCY NAME(S) AND ADDRESS(ES)</b> National Aeronautics and Space Administration Washington, DC 20546-0001			<b>10. SPONSORING/MONITORING AGENCY REPORT NUMBER</b>  NASA TM-4386	
<b>11. SUPPLEMENTARY NOTES</b>				
<b>12a. DISTRIBUTION/AVAILABILITY STATEMENT</b>  Unclassified-Unlimited  Subject Category 93			<b>12b. DISTRIBUTION CODE</b>	
<b>13. ABSTRACT</b> (Maximum 200 words) Initial studies of the sensitivities of estimates of particle fluence, absorbed dose, and dose equivalent to fragmentation parameter variations are undertaken by using the Langley Research Center galactic cosmic ray transport code (HZETRN). The new results, presented as a function of aluminum shield thickness, include upper and lower bounds on dose/dose equivalent corresponding to the physically realistic extremes of the fragmentation process and the percentage of variation of the dose/dose equivalent as a function of fragmentation parameter variation.				
<b>14. SUBJECT TERMS</b> Galactic cosmic radiation; Fragmentation; Dose sensitivity studies			<b>15. NUMBER OF PAGES</b> 8	
			<b>16. PRICE CODE</b> A03	
<b>17. SECURITY CLASSIFICATION OF REPORT</b> Unclassified	<b>18. SECURITY CLASSIFICATION OF THIS PAGE</b> Unclassified	<b>19. SECURITY CLASSIFICATION OF ABSTRACT</b>	<b>20. LIMITATION OF ABSTRACT</b>	

## Abstract

*Initial studies of the sensitivities of estimates of particle fluence, absorbed dose, and dose equivalent to fragmentation parameter variations are undertaken by using the Langley Research Center galactic cosmic ray transport code (HZETRN). The new results, presented as a function of aluminum shield thickness, include upper and lower bounds on dose/dose equivalent corresponding to the physically realistic extremes of the fragmentation process and the percentage of variation of the dose/dose equivalent as a function of fragmentation parameter variation.*

## Introduction

Current methods for estimating interplanetary crew radiation exposures resulting from galactic cosmic rays (GCR's) and their concomitant shielding and dosimetry requirements rely on radiation transport computer codes that describe the interactions and propagation of these radiation fields within and through bulk matter (refs. 1 through 9). The dose and dose equivalent are slowly decreasing functions of increasing shield thickness (refs. 3, 4, and 9) because of secondary particle production processes whereby the heavier GCR nuclei are broken up into nucleons and lighter nuclear fragments by nuclear and coulombic interactions with the shield material.

As has been discussed elsewhere (ref. 5), the slow decrease in dose and dose equivalent with increasing shield thickness means that relatively small variations in predicted doses arising from inaccuracies in nuclear fragmentation models may yield large variations in estimated shield thickness. Because of the paucity of experimental measurements of fragmentation cross sections for GCR ions colliding with spacecraft materials, actual variations in estimates of absorbed dose and dose equivalent resulting from the use of particular nuclear fragmentation models cannot be clearly established at this time. Nevertheless, it is possible to use current fragmentation models and transport codes to study the sensitivities of dose and dose equivalent to variations in these fragmentation cross sections. Careful analyses of the extremes of the fragmentation event also permit the estimation of upper and lower bounds on dose/dose equivalent as a function of shield thickness.

Although currently recommended limits are based upon dose equivalent, it is not a good predictor of biological risk for heavy ion exposures. The engineering design of future, deep-space vehicles will be based upon risk models that are more closely related to the linear energy transfer (LET) spectra of the radiation deposited (ref. 7). Therefore, the effects of variations

in the fragmentation cross sections on the predicted LET spectra will ultimately be of great importance.

In this work, initial studies of the sensitivity of predicted fluences, dose, and dose equivalent to variations of the fragmentation cross-section inputs into the GCR transport code HZETRN (ref. 8) are undertaken. The method used is to simultaneously increase or decrease all magnitudes of the fragmentation cross-section inputs by the same fixed percentage. At present we have chosen to use 0.50, 0.75, 1.25, and 1.50 times the nominal values. We have also estimated upper and lower bounds on the dose, dose equivalent, and LET distributions by considering the extremes of the fragmentation event.

## GCR Risk Assessment

The propagation of these GCR radiation fields in shielding is described by a Boltzmann equation derived from mass and energy conservation. Its solutions give particle fluxes and energies everywhere within and exiting the boundaries of the target medium. For GCR particles, the typically large ion kinetic energies allow one to neglect changes in particle direction because of collisions. This process is called a *straight ahead* approximation. The one-dimensional Boltzmann equation is then written as (refs. 2, 8, and 9)

$$\left[ \frac{\partial}{\partial x} + \sigma_i(E) - \frac{\partial}{\partial E} S_i(E) \right] \phi_i(x, E) = \sum_j \sigma_{ij}(E) \phi_j(x, E) \quad (1)$$

In equation (1),  $\phi_i$  is the flux of type  $i$  ions at position  $x$  with motion along the  $x$ -axis and energy  $E$  (in units of  $A$  MeV),  $\sigma_i$  is the corresponding macroscopic nuclear absorption cross section (in units of  $\text{cm}^{-1}$ ),  $S_i$  is the change in  $E$  per unit distance (e.g., the stopping power per unit projectile mass), and  $\sigma_{ij}$  is the cross section (in units of  $\text{cm}^{-1}$ ) for producing ion  $i$  from a collision by ion  $j$ . For the GCR transport problem, the solution is achieved by using the

first two terms of a perturbation expansion in an iterative procedure which effectively sums subsequent generations of reaction products to all orders. The result is (refs. 2 and 8)

$$\begin{aligned} \phi_i(x+h, E) = & \frac{S_i(E_\gamma) P_i(E_\gamma)}{S_i(E) P_i(E)} \phi_i(x, E_\gamma) \\ & + \sum_j \frac{S_j(E_\delta) \sigma_{ij}}{S_i(E) (\sigma_j - \sigma_i)} \left[ \frac{P_i(E_\gamma)}{P_i(E)} \right. \\ & \left. - \frac{P_j(E_\delta)}{P_j(E)} \right] \phi_j(x, E_\delta) \end{aligned} \quad (2)$$

where

$$\left. \begin{aligned} E_\gamma &= R_i^{-1} [h + R_i(E)] \\ E_\delta &= R_j^{-1} [(\nu_i/\nu_j)h + R_j(E)] \end{aligned} \right\} \quad (3)$$

$$P_i(E) = \exp \left[ -A_i \int_0^E \frac{\sigma_i(e)}{S_i(e)} de \right] \quad (4)$$

$e$  is a dummy variable, and  $\nu_i$ , the range scale parameter relation, is given by

$$\nu_i R_i(E) = \nu_j R_j(E) \quad (5)$$

with  $R_i(E)$  denoting the range of ion  $i$  with energy  $E$  and  $A_i$  denoting its mass number. The first term on the right side of equation (2) represents attenuation of the primary ions. The second term on the right side represents production and attenuation of secondaries. The distance  $h$  is usually chosen to be large enough to minimize the number of iteration steps while concomitantly minimizing the error resulting from the neglect of tertiary production in  $h$ . Equation (2) can be used to propagate the solution a distance  $h$  beyond  $x$ . Taking the initial point on the boundary then allows propagation to any arbitrary depth within the interior. Details of the input stopping powers, nuclear absorption, and fragmentation cross sections are given elsewhere (refs. 7 and 8).

Once the particle fluxes for each GCR ion have been determined using equation (2), the absorbed dose is computed from

$$D_i(x, > E) = A_i \int_E^\infty S_i(E') \phi_i(x, E') dE' \quad (6)$$

For risk assessment, the dose equivalent is obtained from

$$H_i(x, > E) = A_i \int_E^\infty Q_{Fi}(E') S_i(E') \phi_i(x, E') dE' \quad (7)$$

where  $Q_F$  denotes the quality factor that relates absorbed dose to risk. These are LET-dependent quantities obtained from ICRP-26 (ref. 10).

## Results

### Sensitivity Studies

Testing of the sensitivities of the predicted dose/dose equivalent to variations of the fragmentation cross sections ( $\sigma_{ij}$  in eqs. (1) and (2)) was accomplished by replacing  $\sigma_{ij}$  in equations (1) and (2) by  $p\sigma_{ij}$ , where the parameter  $p$  was varied as desired. For this study, we chose the values  $p = 0.50, 0.75, 1.00, 1.25$ , and  $1.50$ . Note that this procedure results in a simultaneous, fixed-percentage increase or decrease in the magnitudes of all fragmentation cross-section inputs. Because of the paucity of experimental fragmentation cross-section measurements, a more realistic approach involving variations of individual cross sections was not considered at this time. Such studies should be performed when the experimental data base for a particular target, such as aluminum, is reasonably well known for many of the incident GCR ions.

The results of the sensitivity studies are displayed in tables I through III for the solar minimum GCR environment obtained from the model of Adams (ref. 11). The percentage of deviations from the nominal values ( $p = 1.00$ ) is displayed in figures 1 and 2. For the absorbed dose, which is least sensitive to cross-section variations, the maximum deviation from the nominal value is approximately 3.5 percent for a 50-percent variation in the cross sections. The dose equivalent appears to be somewhat more sensitive in that a 50-percent variation in the fragmentation cross sections yields a maximum variation in the total dose equivalent of approximately 15 percent.

Table III displays estimated integral fluences by particle type for two thicknesses of aluminum shielding spanning the maximum variations in dose and dose equivalent in tables I and II. Note that the total flux variations are on the order of 5 percent for a 50-percent variation in the cross sections. The largest variations in the table for a given particle type (nearly 70 percent) occur for the group of ions with charges between  $Z = 10$  and  $Z = 28$ . Fluence variations as large as approximately 50 percent also occur for the group of ions with charges between  $Z = 3$  and  $Z = 9$  and for alpha particles ( $Z = 2$ ). Because of the larger quality factors associated with these high-LET particles, the greater

variation of the dose equivalent is understandable when compared with the variation of absorbed dose, even though these particles comprise less than 5 percent of the total fluence at these shield depths. The least variation occurs for protons (4 percent or less) and neutrons (8 percent or less) which comprise over 95 percent of the total transmitted fluence at these

depths. Variations in LET spectra, which (except for bounds on dose equivalent versus LET) are not included in this work, may be larger than the dose equivalent variations because of dominance by the high-LET particles. Such studies, which may be relevant to effects on biological systems, should be undertaken in the future.

Table I. Annual Absorbed Dose of Solar Minimum Galactic Cosmic Rays as Function of Fragmentation Parameter Variation and Aluminum Shield Thickness

Shield thickness, g/cm <sup>2</sup>	Annual absorbed dose, cGy, for fragmentation parameters—				
	$0.5\sigma_{ij}$	$0.75\sigma_{ij}$	$1.0\sigma_{ij}$	$1.25\sigma_{ij}$	$1.50\sigma_{ij}$
0	17.06	17.06	17.06	17.06	17.06
1	15.51	15.47	15.43	15.39	15.35
2	15.82	15.75	15.68	15.60	15.53
3	16.01	15.91	15.81	15.71	15.61
4	16.13	16.00	15.88	15.76	15.64
5	16.21	16.06	15.91	15.77	15.64
10	16.26	16.04	15.84	15.64	15.46
15	16.04	15.78	15.55	15.35	15.16
20	15.66	15.40	15.16	14.96	14.78
30	14.68	14.42	14.20	14.02	13.88
40	13.56	13.31	13.11	12.97	12.85
50	12.41	12.16	11.99	11.86	11.76

Table II. Annual Dose Equivalent of Solar Minimum Galactic Cosmic Rays as Function of Fragmentation Parameter Variation and Aluminum Shield Thickness

Shield thickness, g/cm <sup>2</sup>	Annual dose equivalent, cSv, for fragmentation parameters—				
	$0.5\sigma_{ij}$	$0.75\sigma_{ij}$	$1.0\sigma_{ij}$	$1.25\sigma_{ij}$	$1.50\sigma_{ij}$
0	121.7	121.7	121.7	121.7	121.7
1	84.8	84.3	83.8	83.3	82.9
2	82.1	81.2	80.3	79.4	78.5
3	79.3	78.0	76.8	75.6	74.4
4	76.7	75.1	73.6	72.1	70.7
5	74.3	72.4	70.7	68.9	67.3
10	64.8	62.1	59.5	57.2	55.0
15	58.1	55.0	52.2	49.6	47.4
20	53.0	49.7	46.9	44.4	42.3
30	45.4	42.2	39.6	37.5	35.9
40	39.7	36.7	34.5	32.9	31.7
50	34.9	32.3	30.6	29.3	28.5

Table III. Annual Integral Fluences of Solar Minimum Galactic Cosmic Rays as Function of Fragmentation Parameter Variation for Representative Aluminum Shield Thicknesses

Particle type	Annual integral fluences, particles/cm <sup>2</sup> , for fragmentation parameters—				
	$0.5\sigma_{ij}$	$0.75\sigma_{ij}$	$1.0\sigma_{ij}$	$1.25\sigma_{ij}$	$1.5\sigma_{ij}$
Aluminum thickness of 20 g/cm <sup>2</sup>					
$Z = 0$ neutron	$1.24 \times 10^8$	$1.28 \times 10^8$	$1.32 \times 10^8$	$1.36 \times 10^8$	$1.39 \times 10^8$
$Z = 1$ proton	$1.31 \times 10^8$	$1.33 \times 10^8$	$1.35 \times 10^8$	$1.36 \times 10^8$	$1.38 \times 10^8$
$Z = 2$ alphas	$9.26 \times 10^6$	$8.43 \times 10^6$	$7.67 \times 10^6$	$6.99 \times 10^6$	$6.36 \times 10^6$
$Z = 3-9$	$6.85 \times 10^5$	$6.24 \times 10^5$	$5.68 \times 10^5$	$5.17 \times 10^5$	$4.70 \times 10^5$
$Z = 10-28$	$1.42 \times 10^5$	$1.25 \times 10^5$	$1.09 \times 10^5$	$9.62 \times 10^4$	$8.44 \times 10^4$
Total	$2.65 \times 10^8$	$2.70 \times 10^8$	$2.75 \times 10^8$	$2.80 \times 10^8$	$2.84 \times 10^8$
Aluminum thickness of 40 g/cm <sup>2</sup>					
$Z = 0$ neutron	$1.57 \times 10^8$	$1.64 \times 10^8$	$1.70 \times 10^8$	$1.74 \times 10^8$	$1.78 \times 10^8$
$Z = 1$ proton	$1.11 \times 10^8$	$1.14 \times 10^8$	$1.16 \times 10^8$	$1.18 \times 10^8$	$1.19 \times 10^8$
$Z = 2$ alphas	$7.00 \times 10^6$	$5.80 \times 10^6$	$4.80 \times 10^6$	$3.97 \times 10^6$	$3.29 \times 10^6$
$Z = 3-9$	$4.69 \times 10^5$	$3.88 \times 10^5$	$3.21 \times 10^5$	$2.64 \times 10^5$	$2.17 \times 10^5$
$Z = 10-28$	$8.16 \times 10^4$	$6.30 \times 10^4$	$4.86 \times 10^4$	$3.74 \times 10^4$	$2.88 \times 10^4$
Total	$2.76 \times 10^8$	$2.84 \times 10^8$	$2.91 \times 10^8$	$2.96 \times 10^8$	$3.01 \times 10^8$

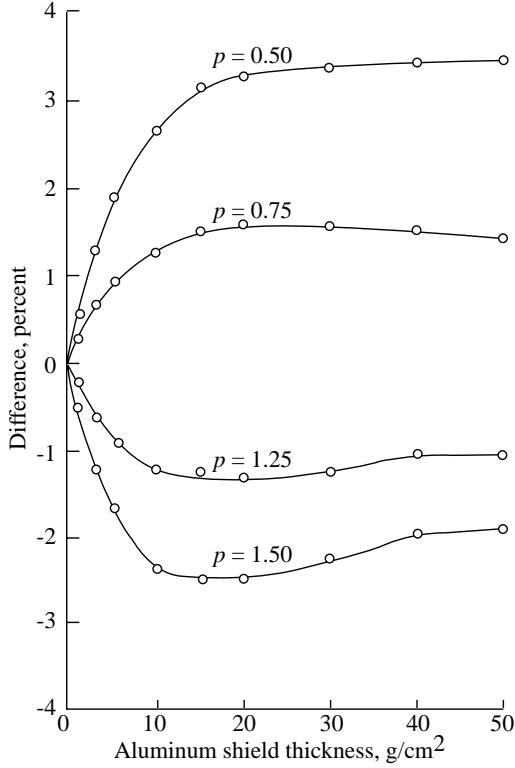


Figure 1. Percentage of difference from nominal values ( $1.0\sigma_{ij}$ ) of absorbed dose as function of aluminum shield thickness. Values are displayed for four different sets of input fragmentation parameters ( $p\sigma_{ij}$ ).

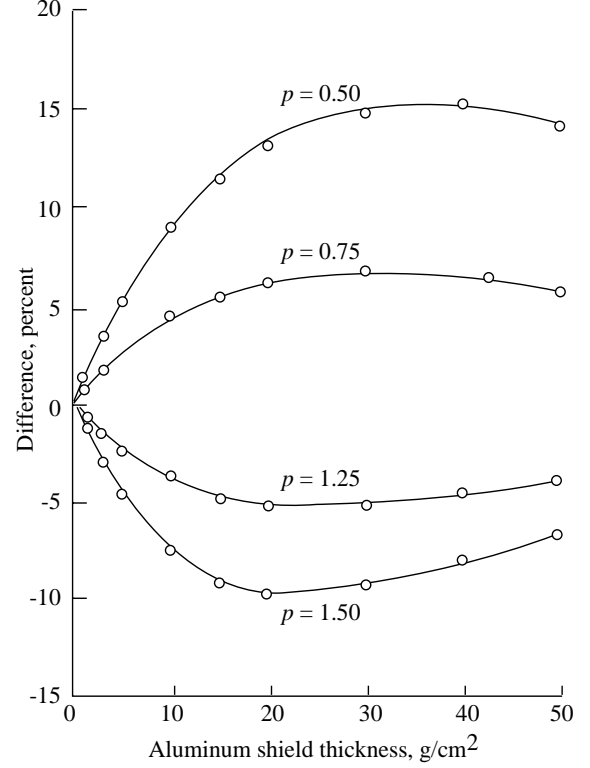


Figure 2. Percentage of difference from nominal values ( $1.0\sigma_{ij}$ ) of dose equivalent as function of aluminum shield thickness. Values are displayed for four different sets of input fragmentation parameters ( $p\sigma_{ij}$ ).

## Maximum and Minimum Bounds

Realistic upper and lower limits on the estimated dose and dose equivalent resulting from variations in the input fragmentation cross sections can be made by considering the extremes of a fragmentation event. The maximum fragmentation event occurs when the projectile nucleus is completely broken up into its constituent nucleons. We call this event the *low-LET* case because there are no heavy-charged particle fragments produced in the reaction. The other extreme, the minimum fragmentation event, occurs when every collision removes only a single nucleon from the fragmenting projectile nucleus. We call this event the *high-LET* case because every reaction produces a heavy-charged particle whose mass number is one unit less than the mass number of the fragmenting nucleus.

To implement this fragmentation model in the Boltzmann equation (eq. (1)), we write the fragmentation cross section as

$$\sigma_{ij} = m_{ij} \sigma_j \quad (8)$$

For the low-LET case, where only neutrons and protons are produced,

$$m_{ij} = \begin{cases} Z_j & (i = 1 \text{ proton}) \\ A_j - Z_j & (i = 0 \text{ neutron}) \\ 0 & (i \neq 0, 1) \end{cases} \quad (9)$$

For the high-LET case, where only a single neutron is removed from the fragmenting nucleus, we use

$$m_{ij} = (A_j - Z_j)/A_j \quad (10)$$

for  $i = j$  and  $i = 0$ ; but for all other events,  $m_{ij} \equiv 0$ . For the high-LET case where a single proton is removed, equation (10) becomes

$$m_{ij} = Z_j/A_j \quad (11)$$

for  $i = j - 1$  and  $i = 1$ ; but for all other events,  $m_{ij} \equiv 0$ . Finally, we note that the values of the absorption cross sections  $\sigma_j$  are known to within approximately 10 percent (ref. 12). Therefore, we also vary  $\sigma_j$  by  $\pm 10$  percent as part of the bounding process.

Figures 3 and 4 display bounds on the absorbed dose and dose equivalent obtained using equations (8) through (11). For aluminum shield thicknesses between 15 and 20 g/cm<sup>2</sup>, differences between the upper and lower bounds on the absorbed dose exceed 6 percent. For aluminum shield thicknesses between 20 and 50 g/cm<sup>2</sup>, differences between the up-

per and lower bounds on the dose equivalent exceed 50 percent.

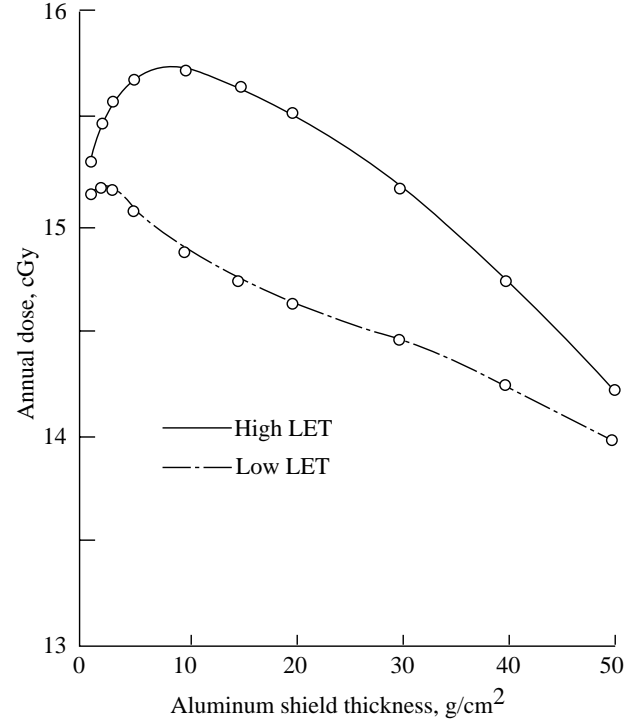


Figure 3. Maximum dose variation in solar minimum galactic cosmic rays resulting from consideration of extremes of fragmentation event. High LET refers to minimum fragmentation event, and low LET refers to maximum event.

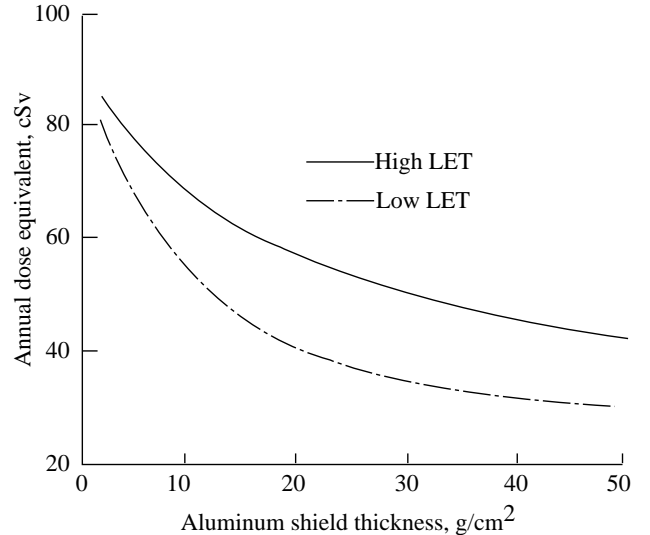


Figure 4. Maximum dose equivalent variation in solar minimum galactic cosmic rays resulting from consideration of bounds of fragmentation events. High LET refers to minimum fragmentation event, and low LET refers to maximum event.

Bounds on the LET distributions behind 5, 10, 20, and 30 g/cm<sup>2</sup> of aluminum shielding are shown

in figures 5, 6, 7, and 8, respectively. For LET values greater than  $10 \text{ keV}/\mu\text{m}$ , differences exceed 20 percent behind  $5 \text{ g}/\text{cm}^2$  of aluminum shielding. Increasing the shielding thickness to  $10 \text{ g}/\text{cm}^2$  of aluminum results in LET distributions that differ by 50 percent or more. These differences increase to greater than a factor of 2 for shield thicknesses exceeding  $20 \text{ g}/\text{cm}^2$  of aluminum.

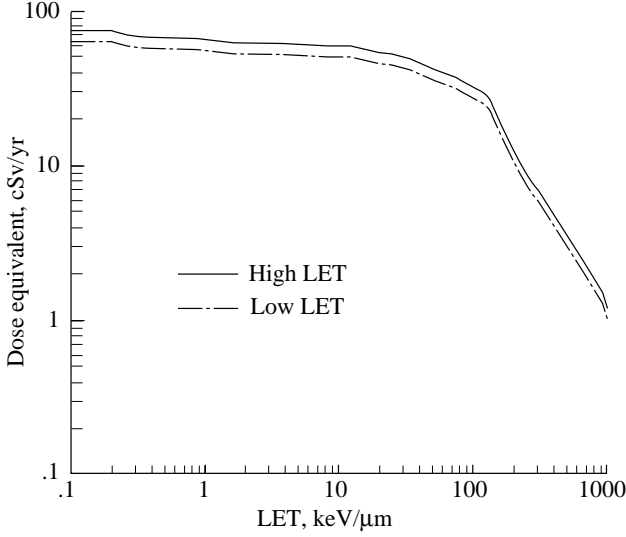


Figure 5. Maximum LET distribution variation in solar minimum galactic cosmic rays behind  $5 \text{ g}/\text{cm}^2$  of aluminum shielding resulting from consideration of bounds of fragmentation event. High LET refers to minimum fragmentation event, and low LET refers to maximum event.

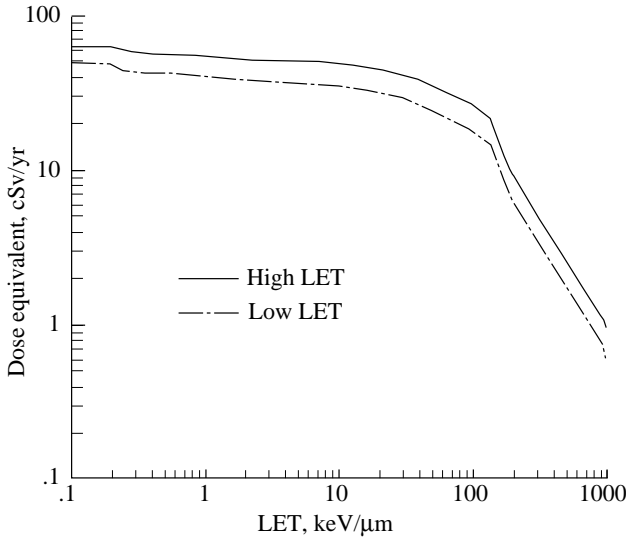


Figure 6. Maximum LET distribution variation in solar minimum galactic cosmic rays behind  $10 \text{ g}/\text{cm}^2$  of aluminum shielding resulting from consideration of bounds of fragmentation event. High LET refers to minimum fragmentation event, and low LET refers to maximum event.

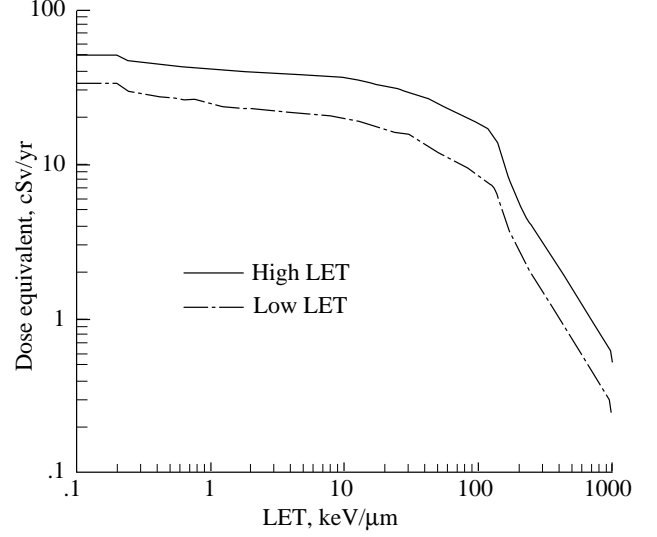


Figure 7. Maximum LET distribution variation in solar minimum galactic cosmic rays behind  $20 \text{ g}/\text{cm}^2$  of aluminum shielding resulting from consideration of bounds of fragmentation event. High LET refers to minimum fragmentation event, and low LET refers to maximum event.

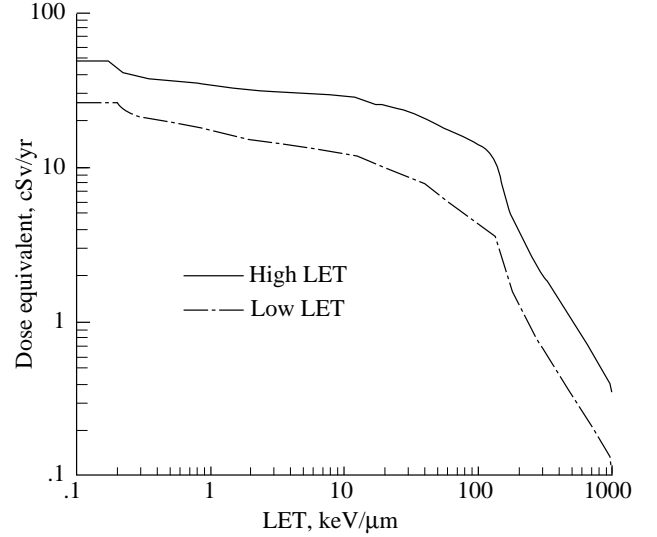


Figure 8. Maximum LET distribution variation in solar minimum galactic cosmic rays behind  $30 \text{ g}/\text{cm}^2$  of aluminum shielding resulting from consideration of bounds of fragmentation event. High LET refers to minimum fragmentation event, and low LET refers to maximum event.

## Recommended Studies

The bounds and sensitivity studies reported herein comprise an *initial* investigation of the effects of fragmentation parameter uncertainties on calculations of galactic cosmic ray exposure. They are by no means exhaustive in nature. The quantitative results obtained from these studies may be peculiar to the

present transport code and its associated inputs. No claim is made that alternative transport codes will yield these exact results. Further studies that should be considered include the following:

1. Incorporating body self-shielding distributions to estimate actual organ exposure uncertainties
2. Estimating exposure uncertainties for other shield materials
3. Expanding the scope of the studies to include the newly proposed quality factors from ICRP-60 (ref. 13)
4. Using other GCR environmental models as they become available
5. Carefully studying the effects of parameter variations on LET distributions.

Finally, whenever complete sets of fragmentation cross-section data relevant to GCR transport in shield materials become available, *actual* estimates of uncertainties in dosimetric quantities should be made.

## Concluding Remarks

Initial studies of the sensitivities of galactic cosmic ray dose and dose equivalent estimates to variations in the input fragmentation cross sections were carried out for typical thicknesses of spacecraft aluminum shielding. Increases as large as 15 percent were noted in dose equivalent when the input fragmentation cross sections were reduced to half of their current values. Variations in absorbed dose were smaller in magnitude and reflected the predominance of high-energy protons in the particle fluence spectra. For particles with charge number  $Z \geq 2$ , large variations in their fluences were noted. These are important because they are the major components of particles of high linear energy transfer (LET).

Upper and lower bounds on dosimetric quantities were established by considering the physical extremes of the fragmentation process. Differences between the upper and lower bounds on dose equivalent exceeded 50 percent for aluminum shield thicknesses greater than 20 g/cm<sup>2</sup>. Above 10 keV/ $\mu$ m, differences exceeding a factor of 2 were noted for the bounds on the LET distributions. Finally, suggestions were made in regard to additional studies needed on fragmentation parameter sensitivity.

## References

1. Heinrich, W.: Calculation of LET-Spectra of Heavy Cosmic Ray Nuclei at Various Absorber Depths. *Radiat. Effects*, vol. 34, 1977, pp. 143-148.
2. Wilson, John W.; and Badavi, F. F.: Methods of Galactic Heavy Ion Transport. *Radiat. Res.*, vol. 108, 1986, pp. 231-237.
3. Wilson, J. W.; Townsend, L. W.; and Badavi, F. F.: Galactic HZE Propagation Through the Earth's Atmosphere. *Radiat. Res.*, vol. 109, no. 2, Feb. 1987, pp. 173-183.
4. Letaw, John R.; Silberberg, Rein; and Tsao, C. H.: Radiation Hazards on Space Missions. *Nature*, vol. 330, no. 6150, Dec. 1987, pp. 700-710.
5. Townsend, Lawrence W.; Nealy, John E.; Wilson, John W.; and Simonsen, Lisa C.: *Estimates of Galactic Cosmic Ray Shielding Requirements During Solar Minimum*. NASA TM-4167, 1990.
6. Townsend, L. W.; Wilson, J. W.; Cucinotta, F. A.; and Shinn, J. L.: Galactic Cosmic Ray Transport Methods and Radiation Quality Issues. *Nucl. Tracks Radiat. Meas.*, vol. 20, no. 1, 1992, pp. 65-72.
7. Wilson, John W.; Townsend, Lawrence W.; Schimmerling, Walter; Khandelwal, Govind S.; Khan, Ferdous; Nealy, John E.; Cucinotta, Francis A.; Simonsen, Lisa C.; Shinn, Judy L.; and Norbury, John W.: *Transport Methods and Interactions for Space Radiations*. NASA RP-1257, 1991.
8. Wilson, John W.; Chun, Sang Y.; Badavi, Forooz F.; Townsend, Lawrence W.; and Lamkin, Stanley L.: *HZETRN: A Heavy Ion/Nucleon Transport Code for Space Radiations*. NASA TP-3146, 1991.
9. Townsend, Lawrence W.; Cucinotta, Francis A.; and Wilson, John W.: Interplanetary Crew Exposure Estimates for Galactic Cosmic Rays. *Radiat. Res.*, vol. 129, no. 1, 1992, pp. 48-52.
10. *Recommendations of the International Commission on Radiological Protection*. ICRP Publ. 26, Pergamon Press, Jan. 17, 1977.
11. Adams, James H., Jr.: *Cosmic Ray Effects on Microelectronics, Part IV*. NRL Memo. Rep. 5901 (Revised), Naval Research Lab., Dec. 31, 1987.
12. Townsend, Lawrence W.; and Wilson, John W.: *Tables of Nuclear Cross Sections for Galactic Cosmic Rays—Absorption Cross Sections*. NASA RP-1134, 1985.
13. *1990 Recommendations of the International Commission on Radiological Protection*. ICRP Publ. 60, International Commission on Radiological Protection, c.1991.

NASA Langley Research Center  
Hampton, VA 23665-5225  
June 23, 1992



Table I. Annual Absorbed Dose of Solar Minimum Galactic Cosmic Rays as Function of Fragmentation Parameter Variation and Aluminum Shield Thickness

Shield thickness, g/cm <sup>2</sup>	Annual absorbed dose, cGY, for fragmentation parameters—				
	$0.5\sigma_{ij}$	$0.75\sigma_{ij}$	$1.0\sigma_{ij}$	$1.25\sigma_{ij}$	$1.50\sigma_{ij}$
0	17.06	17.06	17.06	17.06	17.06
1	15.51	15.47	15.43	15.39	15.35
2	15.82	15.75	15.68	15.60	15.53
3	16.01	15.91	15.81	15.71	15.61
4	16.13	16.00	15.88	15.76	15.64
5	16.21	16.06	15.91	15.77	15.64
10	16.26	16.04	15.84	15.64	15.46
15	16.04	15.78	15.55	15.35	15.16
20	15.66	15.40	15.16	14.96	14.78
30	14.68	14.42	14.20	14.02	13.88
40	13.56	13.31	13.11	12.97	12.85
50	12.41	12.16	11.99	11.86	11.76

Table II. Annual Dose Equivalent of Solar Minimum Galactic Cosmic Rays as Function of Fragmentation Parameter Variation and Aluminum Shield Thickness

Shield thickness, g/cm <sup>2</sup>	Annual dose equivalent, cSv, for fragmentation parameters—				
	$0.5\sigma_{ij}$	$0.75\sigma_{ij}$	$1.0\sigma_{ij}$	$1.25\sigma_{ij}$	$1.50\sigma_{ij}$
0	121.7	121.7	121.7	121.7	121.7
1	84.8	84.3	83.8	83.3	82.9
2	82.1	81.2	80.3	79.4	78.5
3	79.3	78.0	76.8	75.6	74.4
4	76.7	75.1	73.6	72.1	70.7
5	74.3	72.4	70.7	68.9	67.3
10	64.8	62.1	59.5	57.2	55.0
15	58.1	55.0	52.2	49.6	47.4
20	53.0	49.7	46.9	44.4	42.3
30	45.4	42.2	39.6	37.5	35.9
40	39.7	36.7	34.5	32.9	31.7
50	34.9	32.3	30.6	29.3	28.5

Table III. Annual Integral Fluences of Solar Minimum Galactic Cosmic Rays as Function of Fragmentation Parameter Variation for Representative Aluminum Shield Thicknesses

Particle type	Annual integral fluences, particles/cm <sup>2</sup> , for fragmentation parameters—				
	$0.5\sigma_{ij}$	$0.75\sigma_{ij}$	$1.0\sigma_{ij}$	$1.25\sigma_{ij}$	$1.5\sigma_{ij}$
Aluminum thickness of 20 g/cm <sup>2</sup>					
$Z = 0$ neutron	$1.24 \times 10^8$	$1.28 \times 10^8$	$1.32 \times 10^8$	$1.36 \times 10^8$	$1.39 \times 10^8$
$Z = 1$ proton	$1.31 \times 10^8$	$1.33 \times 10^8$	$1.35 \times 10^8$	$1.36 \times 10^8$	
$Z = 2$ alphas	$9.26 \times 10^6$	$8.43 \times 10^6$	$7.67 \times 10^6$	$6.99 \times 10^6$	$6.39 \times 10^6$
$Z = 3-9$	$6.85 \times 10^5$	$6.24 \times 10^5$	$5.68 \times 10^5$	$5.17 \times 10^5$	$4.70 \times 10^5$
$Z = 10-28$	$1.42 \times 10^5$	$1.25 \times 10^5$	$1.09 \times 10^5$	$9.62 \times 10^5$	$8.44 \times 10^5$
Total	$2.65 \times 10^8$	$2.70 \times 10^8$	$2.75 \times 10^8$	$2.80 \times 10^8$	$2.84 \times 10^8$
Aluminum thickness of 40 g/cm <sup>2</sup>					
$Z = 0$ neutron	$1.57 \times 10^8$	$1.64 \times 10^8$	$1.70 \times 10^8$	$1.74 \times 10^8$	$1.78 \times 10^8$
$Z = 1$ proton	$1.11 \times 10^8$	$1.14 \times 10^8$	$1.16 \times 10^8$	$1.18 \times 10^8$	$1.19 \times 10^8$
$Z = 2$ alphas	$7.00 \times 10^6$	$5.80 \times 10^6$	$4.80 \times 10^6$	$3.97 \times 10^6$	$3.29 \times 10^6$
$Z = 3-9$	$4.69 \times 10^5$	$3.88 \times 10^5$	$3.21 \times 10^5$	$2.64 \times 10^5$	$2.17 \times 10^5$
$Z = 10-28$	$8.16 \times 10^4$	$6.30 \times 10^4$	$4.86 \times 10^4$	$3.74 \times 10^4$	$2.88 \times 10^4$
Total	$2.76 \times 10^8$	$2.84 \times 10^8$	$2.91 \times 10^8$	$2.96 \times 10^8$	$3.01 \times 10^8$